EARTH SURFACE PROCESSES AND LANDFORMS
Earth Surf. Process. Landforms (2019)

Published online in Wiley Online Library
(wileyonlinelibrary.com) DOI: 10.1002/esp.4611

Surface melt-driven seasonal behaviour (englacial and subglacial) from a soft-bedded temperate glacier recorded by *in situ* wireless probes

Jane K. Hart,[1]* Kirk Martinez,[2] Philip J. Basford,[2] Alexander I. Clayton,[1†] Graeme M. Bragg,[2] Tyler Ward[2] and David S. Young[2]
[1] Geography and Environment, University of Southampton, Southampton, UK
[2] Electronics and Computer Science, University of Southampton, Southampton, UK

Received 21 April 2017; Revised 7 March 2019; Accepted 11 March 2019

*Correspondence to: Jane K. Hart, Geography and Environment, University of Southampton, Southampton, SO17 1BJ, UK. E-mail: jhart@soton.ac.uk
†Current address: Winchester College, Winchester, UK

ESPL
Earth Surface Processes and Landforms

ABSTRACT: We investigate the spatial and temporal englacial and subglacial processes associated with a temperate glacier resting on a deformable bed using the unique Glacsweb wireless *in situ* probes (embedded in the ice and the till) combined with other techniques [including ground penetrating radar (GPR) and borehole analysis]. During the melt season (spring, summer and autumn), high surface melt leads to high water pressures in the englacial and subglacial environment. Winter is characterized by no surface melting on most days ('base') apart from a series of positive degree days. Once winter begins, a diurnal water pressure cycle is established in the ice and at the ice/sediment interface, with direct meltwater inputs from the positive degree days and a secondary slower englacial pathway with a five day lag. This direct surface melt also drives water pressure changes in the till. Till deformation occurred throughout the year, with the winter rate approximately 60% that of the melt season. We were able to show the bed comprised patches of till with different strengths, and were able to estimate their size, relative percentage and temporal stability. We show that the melt season is characterized by a high pressure distributed system, and winter by a low pressure channelized system. We contrast this with studies from Greenland (overlying rigid bedrock), where the opposite was found. We argue our results are typical of soft bedded glaciers with low englacial water content, and suggest this type of glacier can rapidly respond to surface-driven melt. Based on theoretical and field results we suggest that the subglacial hydrology comprises a melt season distributed system dominated by wide anastomosing broad flat channels and thin water sheets, which may become more channelized in winter, and more responsive to changes in meltwater inputs. © 2019 The Authors. Earth Surface Processes and Landforms published by John Wiley & Sons Ltd.

KEYWORDS: subglacial processes; *in situ* experiments; till; GPR; subglacial hydrology

Introduction

Glacier response to climate change is controlled by the two interactive processes of subglacial sediment deformation and hydrology (Boulton and Jones, 1979; Fountain and Walder, 1998). Surface melting generates melt water, which may travel through the glacier to its base, where it can regulate glacier velocity via sliding and/or till deformation (Iken *et al.*, 1993; Willis, 1995; Hubbard and Nienow, 1997; Zwally *et al.*, 2002; Anderson *et al.*, 2004; Schoof, 2010; Sugiyama *et al.*, 2011; Bartholomew *et al.*, 2012). Although there have been an increasing number of studies of these processes due to a series of new technologies, including *in situ* glacier monitoring (Fischer and Clarke, 2001; Murray and Porter, 2001; Hart *et al.*, 2009), geophysics (Smith, 2006; King *et al.*, 2009; Matsuoka *et al.*, 2010), borehole videos (Fountain *et al.*, 2005; Hubbard *et al.*, 2008) and differential global positioning system (dGPS) (Wiens *et al.*, 2008; Waechter *et al.*, 2015), instrumented data are still rare because of the logistical difficulties in accessing the glacial environment.

Most models of the subglacial environment have assumed a rigid bedrock (Hubbard *et al.*, 1995; Bartholmew *et al.*, 2010; Andrews *et al.*, 2014). However, many of the fast flowing ice streams of Antarctica are resting on unconsolidated sediments (soft bedded) which is important in controlling its stability (Schroeder *et al.*, 2013; Joughin *et al.*, 2014; DeConto and Pollard, 2016), as well as large parts of the Quaternary Ice sheets of Europe and North America (Boulton and Hindmarsh, 1987; Hicock and Dreimanis, 1992; Hart *et al.*, 2011).

When a glacier rests on unconsolidated material, subglacial deformation is very common, with 20–85% of glacier motion occurring within the subglacial sediment layer (till) rather than the ice (Boulton *et al.*, 2001), and deformation in this layer can be modelled as a shear zone (Hart and Boulton, 1991).

Pore-water pressure is an important factor in determining subglacial processes and the resultant sedimentation (Boulton and Jones, 1979; Alley *et al.*, 1986; Clarke, 1987; Brown *et al.*, 1987; Hart and Boulton, 1991; Hicock, 1992; Hicock and Dreimanis, 1992; Iverson, 2010).

The glacier bed will comprise a mosaic of different strengths, comprising weak 'slippery' spots and stronger 'sticky' spots (Alley, 1993; Piotrowski *et al.*, 2004; Stokes *et al.*, 2007, 2009; Trommelen *et al.*, 2014) and these subglacial processes can change both temporally and spatially (Smith and Murray, 2009; Hart *et al.*, 2011).

Unconsolidated beds will also have a different type of subglacial hydrology. Instead of a channelized system (Röthlisberger, 1972; Nienow *et al.*, 1998), the subglacial water will flow through a combination of a braided/swampy/canal system alongside a thin macroporous layer (Weertman, 1964; Hooke *et al.*, 1990; Kamb, 1991; Hock and Hooke, 1993; Walder and Fowler, 1994; Creyts and Schoof, 2009; Schroeder *et al.*, 2013).

It has been argued that enhanced temperature rise in the Arctic ('Arctic Amplification' – Serreze and Francis, 2006; Solomon et al., 2007; Cohen *et al.*, 2014) will lead to increased surface melting, resulting in increased basal sliding, which brings more ice into lower altitudes, which accelerates further melting (Zwally *et al.*, 2002; Joughin *et al.*, 2008; Shepherd *et al.*, 2009). However, there is an alternative model that suggests that increases in melt do not necessarily lead to faster glacier velocities (Sundal *et al.*, 2011; Sole *et al.*, 2013; Tedstone *et al.*, 2015). These researchers argue that in early summer, meltwater causes increased storage and higher water pressures. Once channelization occurs, this increases drainage capacity and decreases water pressure, and so the subglacial hydrological system can accommodate increased melt.

There have been fewer studies of the effect on increased surface melting on the behaviour of glaciers with unconsolidated beds. In this study we present an instrumented data set from an Icelandic temperate soft bedded glacier, to investigate water pathways through the ice and the till, to understand a multi-year seasonal response to surface melt and to determine to what degree do water pressure variations moderate ice flow.

Field Site and Previous Studies

The study was undertaken at Skálafellsjökull, Iceland (Figure 1a), an outlet glacier of the Vatnajökull icecap which rests on Upper Tertiary grey basalts. The area of the glacier is approximately 100 km^2 with a length of 25 km (Sigurðsson, 1998). The study site was located on the glacier at an elevation of 792 m above sea level (a.s.l.), where the ice was flat and

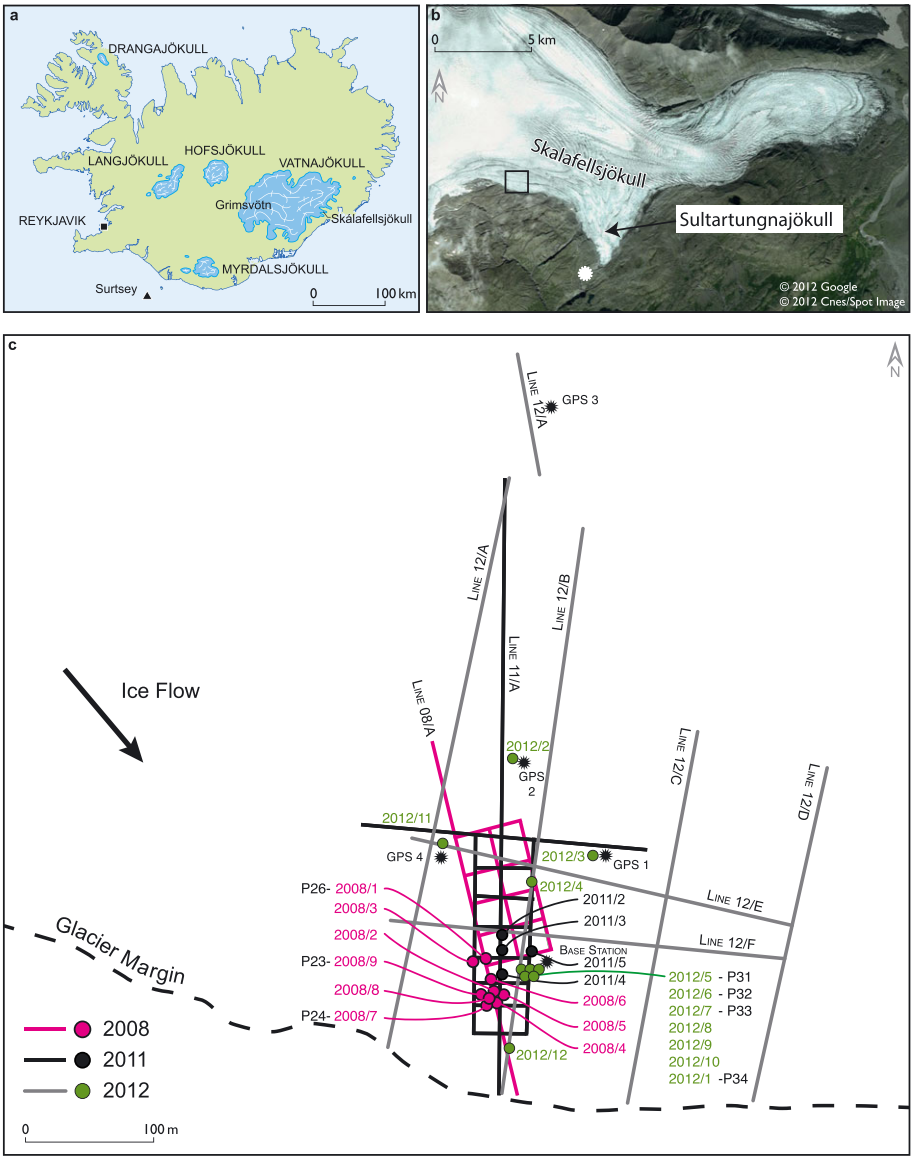

Figure 1. Skálafellsjökull: (a) location in Iceland, (b) details of the glacier, (c) borehole locations (circles) and ground-penetrating radar (GPR) survey grids (lines). [Colour figure can be viewed at wileyonlinelibrary.com]

crevasse free. The subglacial meltwater in this area emerges 3 km away at the southern part of the glacier (known as the Sultartungnajökull tongue, Figure 1b).

The site was examined for five years 2008–2012 and previous studies (Hart *et al.*, 2015, 2018) have shown the following:

a. A fine-grained till (mean grain size 53 µm) covered the majority of the glacier bed.
b. There was evidence of subglacial deformation in the foreland, comprising flutes and push moraines.
c. The data from boreholes (26–86 m in depth) were similar each year and showed that the majority (15 out of 19) remained filled with water during and after drilling. Video evidence showed only one borehole with englacial drainage, two with subglacial cavities, and one with fast flowing water (subglacial channel).
d. Repeat ground-penetrating radar (GPR) surveys (combined with measured glacier depth and video recordings) showed that the glacier had a low water content (0.54% ± 0.26), and that the majority of the glacier had a mean radar velocity of 0.177 ± 0.005 m ns^{-1}, with a thin 1 m debris-rich basal ice layer with a radar velocity of 0.158 ± 0.003 m ns^{-1}.
e. The GPR results from 2008 and 2011 were used to reconstruct the nature of the bed from basal reflection strength.

It was concluded that the glacier has little englacial storage, the ice was impermeable and drainage pathways were concentrated in fractures and moulins. GPR results combined with modelling showed that the subglacial hydrological systems comprised a series of subglacial braided water bodies flowing parallel with the glacier margin.

Methodology

The Glacsweb system

A key component of the data collection is the Glacsweb environmental sensor network (Hart and Martinez, 2006) which comprises sensor nodes (probes and geophones), base stations and a sensor network server in the UK, linked together by radio (Figure 2). Sensors within a probe (0.16 m long, axial ratio 2.9:1), measured water pressure, force, resistance, tilt and temperature within the ice or till. These data were recorded every 15 minutes in 2012 and every hour 2008–2010, and transmitted (via 151 MHz radio) to a base station located on the glacier surface. Probe data, along with dGPS and meteorological data, were sent once a day to a mains powered computer (2.5 km away), where it was forwarded to a web server (via a GPRS link) in the UK (Table I). Details of the 2008–2010 system are discussed in Martinez *et al.* (2009) and the 2012 system in Martinez *et al.* (2012). This system can only transmit through 70 m of ice, however dGPS measurements of annual surface velocity (discussed in more detail later) show a positive relationship between velocity and depth (r^2 = 0.98), indicating that the ice at the study site is representative of glacier motion as whole (Figure 3).

Probes

These were deployed in the summers of 2008 and 2012, in a series of boreholes (57–69 m in depth), which were drilled with a Kärcher HDS1000DE jet wash system (Figure 1c). The depths of the boreholes were measured to calculate glacier thickness. The glacier and till were examined using a custom made digital infrared light-emitting diode (LED) illuminated colour video camera, via the borehole.

In order to insert probes into the till, the boreholes were drilled to the base of the glacier and the presence of till checked with the video camera. If till was present it was hydraulically excavated (Blake *et al.*, 1992) by maintaining the

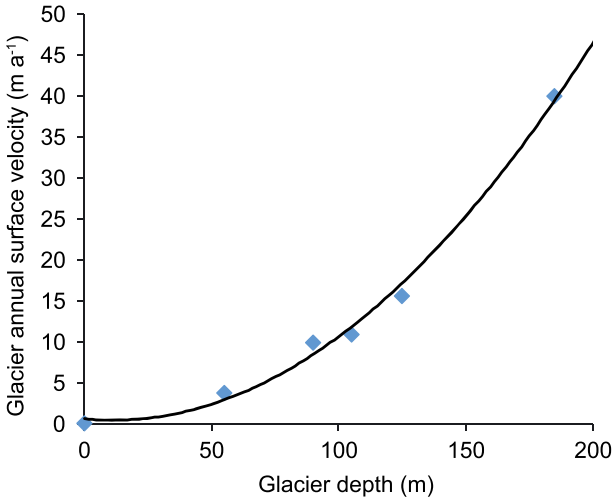

Figure 3. Surface horizontal velocity against glacier depth. [Colour figure can be viewed at wileyonlinelibrary.com]

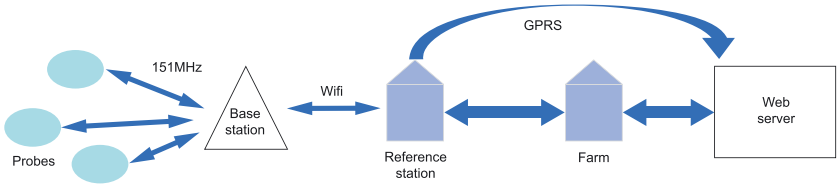

Figure 2. Glacsweb sensor network system. [Colour figure can be viewed at wileyonlinelibrary.com]

Table I. Sensors in the Glacsweb probes

	2008			2012		
	Technical specifications	Resolution (step size)	Range	Technical specifications	Resolution (step size)	Range
Temperature sensor	DS1631	0.0625°C	–10 to +85°C	INA333 custom	0.002°C	± 5°C
Pressure transducer	24PCGFM6G	1.122 kPa	0–1724 kPa	Honeywell 19c200pa7k	0.83 kPa	0–1380 kPa
Strain gauges	Strain gauge	1.25 N	0–213 kN	Strain gauge	1.25 N	0–213 kN
Conductivity	Resistance bridge	0.005 µS	0–100 µS	Resistance bridge	0.005 µS	0–100 µS
Tilt sensors 1 and 2	LIS3LV02DQ	0.000976 g	± 2 g	MMA8451Q HMC5883	0.000976 g	± 2 g

jet at the bottom of the borehole for an extended period of time. The probes were then lowered into this space, enabling the till to subsequently close in around them. The measured depth of the probes within the till is not known, but is approximated at 0.1–0.2 m beneath the glacier base, estimated from video footage of the till excavation prior to deployment.

Table I shows the details about the probe sensors. Water pressure was measured in metres water equivalent (m WE) and calculated as a percentage of glacier thickness. The glacier thickness was determined from the GPR and GPS results. The water depths were calibrated against the measured water depths in the borehole immediately after probe deployment.

The conductivity of the material outside the probe was measured across two bolts mounted in the case. This data was used to determine the nature of the material surrounding the probe. The sensors were calibrated in the laboratory. High values indicate wet sediments, and low values indicate dry or frozen material. Probe temperature values were also calibrated in the laboratory using a commercial temperature reference instrument.

Strain gauges measure relative compression and extension of the probe case in two perpendicular planes (case stress) expressed as the force applied to the probes per unit area (in kilopascals). The applied force was calibrated using an Instron 5560 tension/compression machine attached to a nitrogen cooled chamber, where the average chamber temperature was 1.3°C. The chamber was pre-cooled with liquid nitrogen then left to settle around 0°C to be representative of expected basal temperatures.

The Glacsweb probes measure tilt with two dual axis 180° microelectromechanical system (MEMS) accelerometers. Values of 0° *x*-tilt and *y*-tilt represent the probe standing vertically, these were calibrated in the laboratory, and dip was calculated by trigonometry. The probe is normally almost vertical during deployment and inclines towards the horizontal as the glacier moves over the till. We define this decrease in dip as synthetic, and movement in the opposite direction (increases in dip) as antithetic.

Ground penetrating radar (GPR)

Common offset (CO) surveys were carried out over the survey grids in 2008, 2011 and 2012 (Figure 1c). The data was used to calculate radar velocity and water content (reported earlier), and the nature of the bed from the strength of the basal reflection (reported from 2008 and 2011). Here we calculate the bed reflection strength from the 2012 data and compare it with the 2008 and 2011 results to show how basal reflection strength varies in space and time. The surveys used a Sensors and Software Pulse Ekko 100 with a 1000 V transmitter system and 50 MHz antennas. A 2 m antenna spacing and 0.5 m sampling interval were used for the CO survey. A sledge was constructed to hold the antennae at the correct distance apart and allow the system to move along the grid transects more readily.

A series of standard processing steps were applied to the CO survey data using the software package ReflexW (Moorman and Michel, 2000; Murray *et al.*, 2000). Low frequency noise was eliminated (de-wow filter) and a SEC (spreading and exponential compensation) gain was applied to compensate for signal loss with depth. Next a diffraction stack migration and topographic correction were applied. The ice-bed interface was identified manually in radar echograms from a clear strong reflector. It was then possible to calculate the radar-wave velocity in the whole ice column (v) by comparing the return time of the glacier bed in radar echograms (t) with measured borehole glacier depths (h) according to the equation:

$$v = \frac{2h}{t} \quad (1)$$

Subsequently, the GPR data were analysed in order to calculate basal reflection to reconstruct the nature of the bed (Gades *et al.*, 2000; Winebrenner *et al.*, 2003; MacGregor *et al.*, 2007; Matsuoka *et al.*, 2010; Jacobel *et al.*, 2009, 2010). In summary, the power of electromagnetic energy returned from the subglacial interface is determined by three factors: the dielectric properties of the reflector (the basal reflectivity) (R), losses due to geometric spreading (which are related to glacier depth), and losses due to dielectric attenuation within the ice (L_a). We calculate a mean attenuation value (see Hart *et al.*, 2015, for details), and apply this as the best-fit line to the data, as returned power verses depth. The distance from the fitted line is a measure of relative basal reflectivity for each point (Jacobel *et al.*, 2009, 2010). These values were plotted as a histogram and three peaks are identified and these were used to quantify bed strength (see figure 6 in Hart *et al.*, 2015).

Weather data

These were obtained from a meteorological station (Davis Vantage Pro) (temperature, rainfall, wind speed and humidity) sited on the reference station and, during periods of mechanical failure, from a transfer function applied to data from the neighbouring Icelandic meteorological station at Höfn. Daily melt was calculated by the positive degree day algorithm (Braithwaite, 1995; Hock, 2003) using degree day factors for Satujökull, Iceland (Johannesson *et al.*, 1995), 5.6 mm $d^{-1}°C^{-1}$ for snow and 7.7 mm $d^{-1}°C^{-1}$ for ice. Albedo was calculated from the MODIS data, using the threshold between ice and snow to be 0.45, on a 30 m × 30 m grid ASTER digital elevation model (DEM).

Differential global positioning system (dGPS)

A kinematic dGPS was used to map the glacier margin, boreholes, base station and radar grids. In order to measure surface velocities, a Topcon dGPS was used (2008–2012), with four additional dual frequency Leica dGPS stations installed on the glacier (GPS 1–4) in the study area, with a local base station on the moraine (2012–2013) (Figure 1c). These measured at 15 second sampling rate continuously during the melt season and two hours a day during the winter. The GPS data was processed using TRACK (v. 1.24), the kinematic software package developed by Massachusetts Institute of Technology (MIT) (http://www.unavco.org/, http://geoweb.mit.edu/~tah/track_example/).

Data and Results

Weather results

We define the seasons based on the melt rate/air temperature. The melt season comprises spring, summer and autumn [approximate day of year (DOY) 121–289] when there is constant melt on the glacier surface. During winter, there is no surface melt on the majority of days (negative degree days) apart from a series of warmer days when temperatures rise above zero (positive degree days).

Probe data results

The overall results from the probe data collection are shown in Table II and the data from probes with a water pressure record (2008/2010 probes) are shown in Figure 4 which we will discuss in detail. In 2008, six probes were deployed, and four continued to send data after one day. Of these, one probe (Probe 26) was in a borehole that was not drilled to the glacier bed and so was known to be in the ice. The other three were deployed into the till as discussed earlier (Probe 21, Probe 24 and Probe 25). The 2008 probes sent back data for two years with 141 380 readings in total. All the sensors worked apart from the tilt sensors. However in 2009, the software was de-bugged, which enabled the tilt to be read once a day at mid-day.

The probes were designed so that if the data were not immediately accessed then they were stored for later retrieval. There were some problems with communications between the probes and the base station which unfortunately led to the probes filling their programmable memory (EPROM), resulting in some data gaps (Figure 4).

In 2012, four probes were deployed which all functioned. Two of the probes (Probe 31 and Probe 32) were deployed in boreholes that reached the bed (till probes), and Probe 33 was deployed in a borehole that did not reach the bed (ice probe). Probe 34 was installed on a wire as a 'relay' probe in the ice. Although this probe could not move freely, it could record other properties of the ice. The 2012 probes lasted for 15 weeks. There were some sensor failures (particularly the water pressure and conductivity), however 296 235 data points were received from the probes.

After deployment, the probes become embedded into the till as the glacier moves over the initial location of the probes and the boreholes slowly close. For Probe 25, at the beginning of the record (DOY 223–307), water pressure falls were accompanied by a rise in probe temperature and fall in conductivity. This may reflect short periods of connection with the subglacial hydrological system, leading to water pressure decline combined with warmer water entering the till (from its surface source) whilst the borehole was still open and connected to the base. The other probes were incorporated much faster (approximately 15 days). Further discussions of the probe data will not include the days prior to incorporation.

Velocity data

Detailed velocity data was collected 2012–2013 and is shown plotted against surface melt and the continuous tilt data (Figure 5). During the summer, there is no statistical correlation between air temperature and velocity, although the extremes in temperature correlate with the extremes in velocity. However, during the winter there is a different pattern. There is a 'base' velocity during the negative degree days, and velocity peaks during the positive degree days (speed-up events). Although we only have detailed velocity data for 2012 to 2013 we can assume that these speed-up events also occurred in previous years during the positive degree days.

GPR results

The GPR results can be used to calculate the strength of the glacier bed reflection. The results from the 2008 and 2011 surveys were reported in Hart *et al*. (2015), and the same techniques are used to analyse the 2012 data. Using the method of Jacobel *et al*. (2009, 2010) the reflection values were divided into three classes: low reflection values (R) less than −3 dB (indicative of

Table II. Summary of the mean annual probe data in the ice and the till – mean (standard deviation as a percentage of the mean)

Ice					Till						
										Mean tilt changes per day (deg)	
Probe number	Case stress (kPa)	Temp. (°C)	Water pressure (m WE% depth)	Conductivity (ohms)	Probenumber	Case stress (kPa)	Temp.(°C)	Water pressure (m WE% depth)	Conductivity (ohms)	Melt season	Winter
P26	388.43(0.11%)	–0.048(62%)	79.38(23%)	5.54(97%)	P21 Yr 1	253.95(2%)	0.0033 (425%)	95.35 (2%)	8.2 (29%)	—	—
					P21 Yr 2	272.69(10%)	0.0047(352%)	78.46(9%)	27(13%)	0.198	0.101
					P24	224.05(6%)	–0.1108(24%)	86.30(32%)	10.66(93%)	—	—
					P25 Yr 1	298.37(2%)	0.014 (185%)	49.67(53%)	2.78(85%)	—	—
					P25 Yr 2	307.31(0.4%)	0(0.002)	49.50(9%)	10.03(4%)	0.025	0.014
P33	1810.5(5%)	–0.56(11%)	22.26(3%)	—	P31	17.39(11%)	–0.179 (108%)	—	—	0.082	0.078
P34	—	–0.56(10%)	—	—	P32	182.95(19%)	–0.66 (380%)	—		0.112	0.053
Mean	1099.2	–0.304	50.82	5.54	Mean	222.38	–0.132	71.85	11.73	0.104	0.0615

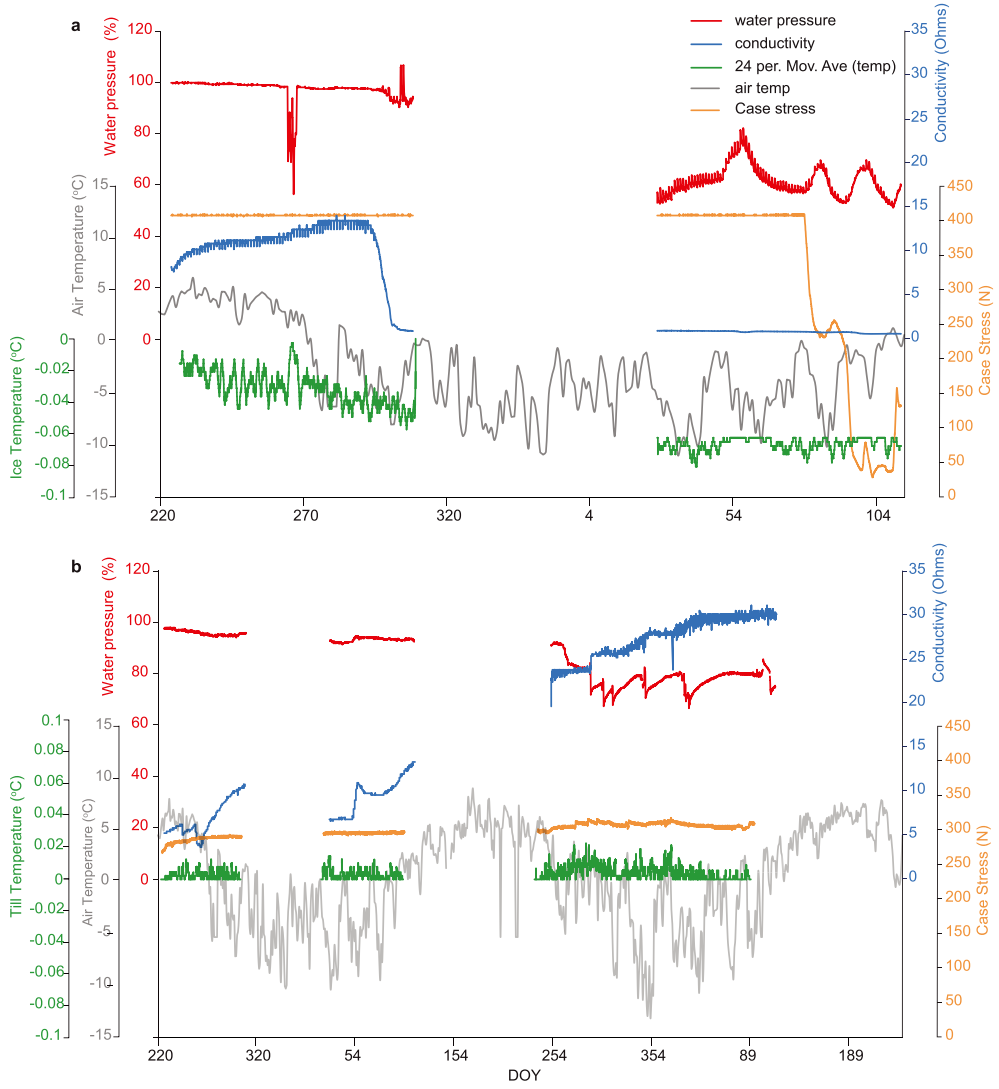

Figure 4. Probe data from 2008 to 2010: (a) Probe 26 deployed in the ice, (b) Probe 21 deployed in the till; (c) Probe 25 deployed in the till, (d) Probe 24, deployed in the till. [Colour figure can be viewed at wileyonlinelibrary.com]

dry till or bedrock), intermediate reflection −3 to 10 dB (indicative of wet till), and high reflection greater than 10 dB (indicative of a water body). We then calculate the percentage of each of these categories along the survey grids (Table III). Areas with low reflectivity/stiffer till or bedrock covered 19%; areas with high reflectivity/water bodies covered 4%; with the remainder (77%) representing the deforming bed. These percentages were consistent for different years, and where repeat surveys were made over the same area, the bed types remained the same.

We are also able to calculate the size of the different patches (also shown in Table III). Over the three surveys, the mean length of the deforming bed areas was 7.9 m, the length of the low reflectivity areas was 2.2 m, and the length of the high reflectivity areas was 1.9 m. These values were very similar each year and demonstrate the scale of the patchwork elements.

Discussion

We now discuss the evidence for spatial and temporal changes in the englacial and subglacial environment, and compare these results with reported *in situ* water pressure data from Greenland.

The englacial environment

The data from Probe 26 shows an excellent example of the behaviour of the englacial environment (Figure 4a). During the summer and autumn most sensor readings remained fairly constant. In Probe 26 water pressure remained high except for DOY 265–267 where there was a decrease in water pressure, accompanied by a rise in probe temperature (Figure 4a).

In contrast, during the winter sensor readings were more variable. Beginning DOY 292 the water pressure began to have a diurnal pattern that continued until the end of the record. This pattern commenced once melting ceased at the glacier surface. This comprised a peak at 13:00 followed by a slow decline. After each positive degree day melt event there was an immediate (but) slow rise in water pressure which reached a peak (12% increase) after approximately five days. There was an inverse relationship between air temperature/melt during the melt event and the resultant peak in water pressure five days later (r^2 = 0.8065). There was also a drop in conductivity as winter began (DOY 292), and this remained low throughout the winter.

Case stress remained constant (and high) until DOY 79 when there was a dramatic decrease, and after that the case stress was very variable, with the largest changes on the day or the day after a peak in meltwater. DOY 79 was the warmest day since the

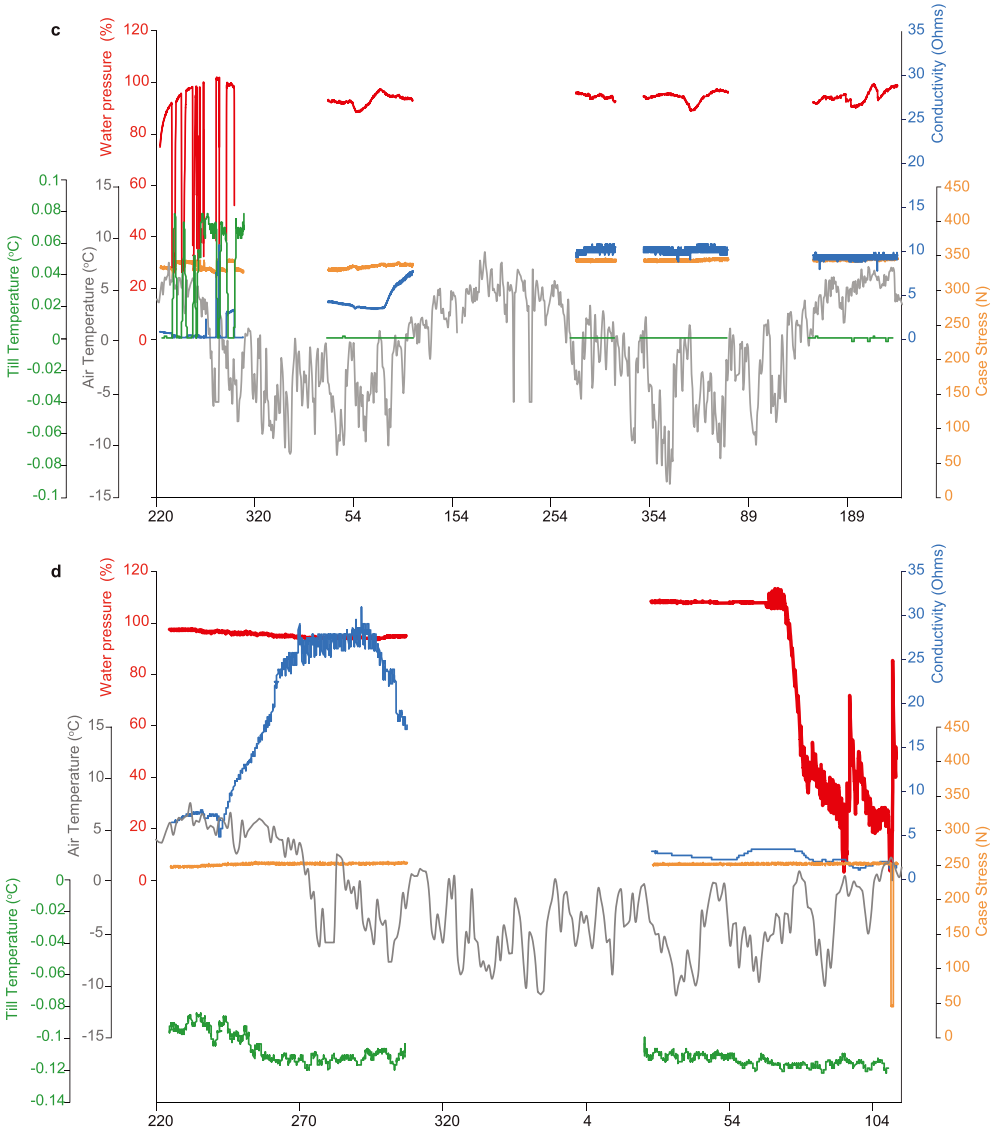

Figure 4. (continued)

previous November. There was also a rise in probe temperature during the high water pressure events.

The GPR evidence showed a low water content, and borehole videos showed no fractures or conduits intersecting the borehole, which suggests the system was relatively closed. It could be argued that the melt season water pressure stability was because the borehole remained full of water (from the drilling) and was unable to drain (DOY 220–291). However, immediately once winter began (i.e. negative degree days) a diurnal cycle commenced (DOY 292–112), water pressure declined and there developed an immediate but slow response to positive degree day events. This implies that the borehole was connected with the englacial or subglacial system. During the melt season, inputs must be equal or greater than outputs to preserve the water pressure stability. But once surface inputs were stopped, during winter, water pressure decreased and the only water sources must be within the ice. Since there is a diurnal change (and winter diurnal rises in discharge were recorded (Young *et al.*, 2015), these sources must be a combination of the release of storage (Rennermalm *et al.*, 2013; Schoof *et al.*, 2014), as well as melt generated from glacier movement. This 'new' water has much lower conductivity (due to dilution) and higher temperatures.

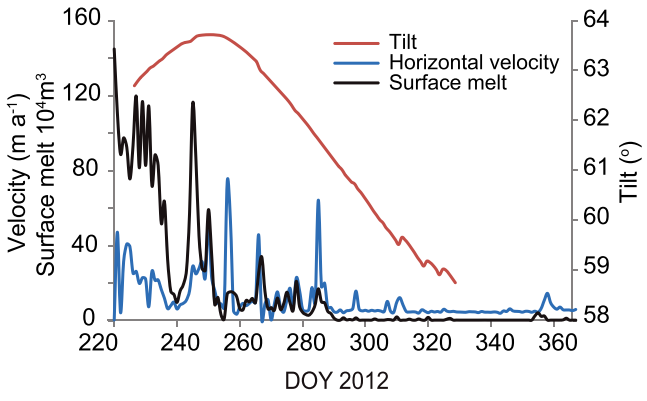

Figure 5. Graph showing the mean daily horizontal surface velocity, tilt and surface melt 2012. [Colour figure can be viewed at wileyonlinelibrary.com]

Numerous researchers have discussed how water travels through the ice. Flux through veins is negligible as ice has a very low permeability (Fountain and Walder, 1998; Gulley *et al.*, 2009). Raymond and Harrison (1975) reported millimetre scale passages, whist Hodge (1976), Pohjola (1994) and Harper and Humphrey (1995) reported passages 0.1 m in scale with an estimated flow of 0.01 to 0.1 m s^{-1}. We recorded very few englacial passages; only 5% (one out of 19) of boreholes intersected with a fracture and/or conduit. This was much lower than others

Table III. Percentage cover and average (and maximum) length of reflection (*R*) values (see text for details)

Year	High *R*			Intermediate *R*			Low *R*		
	% cover	Mean	Maximum	% cover	Mean	Maximum	% cover	Mean	Maximum
2008	3.4%	2.7 m	10 m	70.0%	9.0 m	101 m	26.6%	3.1 m	28 m
2011	6.0%	4.0 m	14 m	84.0%	11.9 m	84 m	11.0%	2.2 m	13 m
2012	3.5%	1.4 m	8 m	75.5%	6.7 m	110 m	21.0%	2.0 m	15 m
All	4.0%	1.9 m	14 m	77.0%	7.9 m	110 m	19.0%	2.2 m	28 m

figures reported from mostly temperate rigid bedded glaciers. Fountain and Walder (1998) described from a range of glaciers that approximately 50% of boreholes drained before the bedrock was reached, indicating the presence of englacial passages. In addition, Fountain *et al.* (2005) reported, from video images of 48 boreholes from Storglaciären, Sweden, that 78% intercepted englacial passages of which most were fractures. However, it is possible that millimetre scale passages or crevasses were present at Skálafellsjökull which were too small to observe on the video images.

The subglacial environment

Probes 21 and 25 (in the till) showed a similar pattern to each other (Figures 4b and 4c). Water pressure was generally high and either stable or variable. Case stress was intermediate and had an inverse relationship with water pressure. The conductivity at the beginning of the record was low and then increased (indicative of wet sediments). The stable water pressure pattern may reflect a lack of connection with the subglacial drainage system (Murray and Clarke, 1995; Kavanaugh and Clarke, 2001; Nienow *et al.*, 2005). These locations could represent 'islands' of high pressure located away from the main drainage systems. In contrast, the variable water pressure pattern may indicate a connection with the subglacial water system), similar to that suggested by Hubbard *et al.* (1995) ('variable pressure axis') and Gooseff *et al.* (2002).

The style of variable water pressure varied between the seasons. This is clearly illustrated from Probe 25 (Figure 4c). During the melt season 2010 there was variation in water pressure, but there was no relationship between water pressure and surface melt. This was in complete contrast to the winter events. In winter 2009 Probe 25 showed a distinct drop in water pressure immediately after the only two positive degree days (DOY 52 and 80). This also occurred during winter 2009/2010. These later events are seen more clearly in Probe 21 during 2009/2010. In that winter, every time air temperatures rose above 2.0°C at the Base Station, water pressure dramatically decreased. This was accompanied by a rise in case stress.

We argue that the overall nature of the water pressure record (stable or variable) was due to the location of the probe in relation to the drainage system. For those probes undergoing variable water pressure changes, these changes were not related to melt during the melt season, but were related to melt during the winter. In addition, during the winter, these melt events are accompanied by speed-up events.

We suggest that the continuous change in tilt that was recorded during the melt season reflects deformation within the till. This deformation was continuous throughout the year, although slower in winter. These results are similar to those from Hart *et al.* (2009) from Briksdalsbreen, where there was also continuous rotation of the probe through the year, with a rate related to glacier surface velocity.

We determined the strength of the bed at the initial probe deployment sites by taking the mean of a 2 m^2 area around the location to allow for error. They all fell within the intermediate bed reflection range, which we have interpreted as deforming till. Results from the tilt data (Table II) showed that although each probe moved at a different rate, there was a generally similar pattern. During the melt season, there was a continuous change in tilt (average 0.1° per day). During the winter, the tilt change was reduced to 60% of the melt season rate. The winter base velocity was also similarly 63% of the melt season mean velocity. The major difference however, was that in winter there were distinct oscillations in tilt (superimposed on the general trend), which occurred during the positive degree days (Figure 5).

Spatial data on the nature of the bed was provided by the GPR data. This showed the widespread presence of a saturated till bed (77% of glacier bed, typically 8 m in length). This remained relatively constant 2008–2012. We use all this evidence to suggest that there was a deforming bed beneath the study area, which was active throughout the year.

The ice/till interface

Probe 24 had a very different record from the three others discussed in detail (Figure 4d). This probe was initially deployed in the till, and the first part of its record (DOY 202–307) was very similar to that of Probe 21, with high and stable water pressures, intermediate and stable case stress, and increasing conductivity. However, when data returns (DOY 27–66) water pressures were over 100% (mean 108%) (and this is the only time in the record any probe showed this), the case stress remained similar, but the conductivity was much lower. On DOY 67 (unrelated to any melt event) a water pressure diurnal cycle was initiated, and water pressures rose to over 113% (case stress rose slightly to 236.6 N); then after DOY 75 water pressures responded directly to melt events (combined with a diurnal cycle). Conductivity rose after DOY 50, and then experienced a small rise during the extreme high water pressures (DOY 67–75) (3.64–3.68 ohms), and then decreased and had an inverse relationship with water pressure until the end of the data series.

At Briksdalsbreen no diurnal cycles were recorded in probes deployed in the till (Hart *et al.*, 2011). Even the till probes at Skálafellsjökull with a variable water pressure record (and assumed to be connected with the subglacial water system), were not variable at the diurnal scale. Therefore, we suggest that when Probe 24 began a diurnal cycle it was connected directly with surface water (since diurnal cycles were recorded in the ice probes), i.e. that it was at the ice/sediment interface.

Since Probe 24 was initially deployed in the till, and during the early part of its record it behaved very similarly to the other till probes with a stable water pressure record (Probe 21), we suggest the following scenario (Figure 6):

a. Sometime between DOY 307 and 27 the water pressure in Probe 24 increased to over 100%. We suggest the probe must be in some type of confined area. Although Murray

and Clarke (1995) argue that greater than 100% water pressures in unconnected areas occur due to low water pressures in connected areas, this is unlikely to explain this situation. We saw no change in water pressure associated with the meltwater event around DOY 50. We suggest the confined area could be a stiffer part of the till, a more clast-rich till, or the probe was held against an obstacle (Figure 6i).

b. Although there was no change in water pressure during the melt event around DOY 50, we can assume there was a speed-up event and there was a subsequent rise in conductivity associated with an increase in wetness. A combination of the sediment change, and glacier speed-up event may have destabilized the probe, and so it subsequently moved on DOY 67 into a location at the ice/sediment interface where it became directly connected to the subglacial water drainage system (hence the diurnal signal). Since the probe water pressure was even higher (and the case stress still high), we suggest that probe remained trapped behind an obstacle at the ice/sediment interface (Figure 6ii).
c. On DOY 75, there was another meltwater driven event (with an associated speed-up), which coincided with the dramatic water pressure and conductivity decrease (Figure 4d). We suggest, due to the associated basal sliding, the probe was moved out of its 'lodged' location, but was still in a connected area at the ice/sediment interface. It may have resided in a microcavity related to the obstacle (Figure 6iii). The reduction in conductivity could result from the till draining or surface meltwater entering the microcavity and causing dilution.
d. The melt events of DOY 75, DOY 93 and DOY 110, were marked by a decrease in water pressure and conductivity. This was followed by a rise in water pressure which peaked five days later, accompanied by continued decreases in conductivity, so the maximum water pressure and minimum conductivity occurred simultaneously with the peak in water pressure in Probe 26. This is further evidence that the probe is now at the ice/sediment interface since it is behaving in a similar way to Probe 26 in the ice.

Contrasting behaviours during the melt season and winter

There are few instrumented studies of the whole glacier (i.e. ice, till and ice/sediment interface) and even fewer during the winter. Here we contrast the behaviour in the three environments.

During the melt season, melt water input into the glacier was high, and equalled or exceeded output. There were no diurnal water pressure changes in the ice. Water pressure in the till was stable or variable related to the location (whether connected or not), but variable water pressures were not related to melt water inputs. The conductivity results in the till from Probe 21 and Probe 25 show that the till remained saturated throughout the season. This accords with the tilt data for constant deformation.

Winter behaviour was very different and was characterized by two distinct regimes, normal 'base' behaviour and melt events. During the melt events, water travelled via different pathways. The first was by direct drainage system through crevasses and moulins, which transported the surface water generated during the positive degree days to the glacier bed, which resulted in basal sliding and glacier speed-up ['fast' direct delivery system discussed by Zwally *et al.*, 2002, Fountain *et al.*, 2005, Das *et al.*, 2008 and Gulley *et al.*, 2009]. This was accompanied by a dramatic fall in water pressure in the till, and change in tilt of the probe.

Some of this water joined the 'indirect' system flowing through the smaller interconnected elements in the englacial

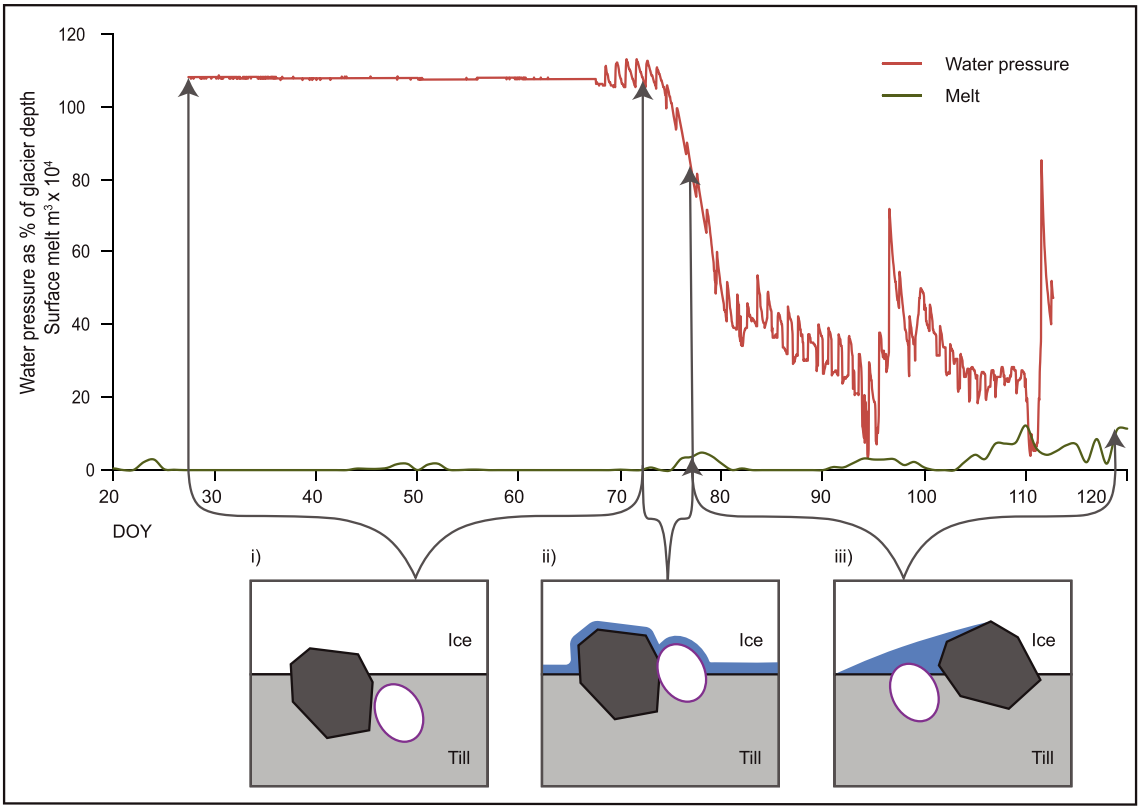

Figure 6. Enlargement of the water pressure and surface melt record for Probe 24 (2009), with the scenarios discussed in the text (ice flow direction from right to left). [Colour figure can be viewed at wileyonlinelibrary.com]

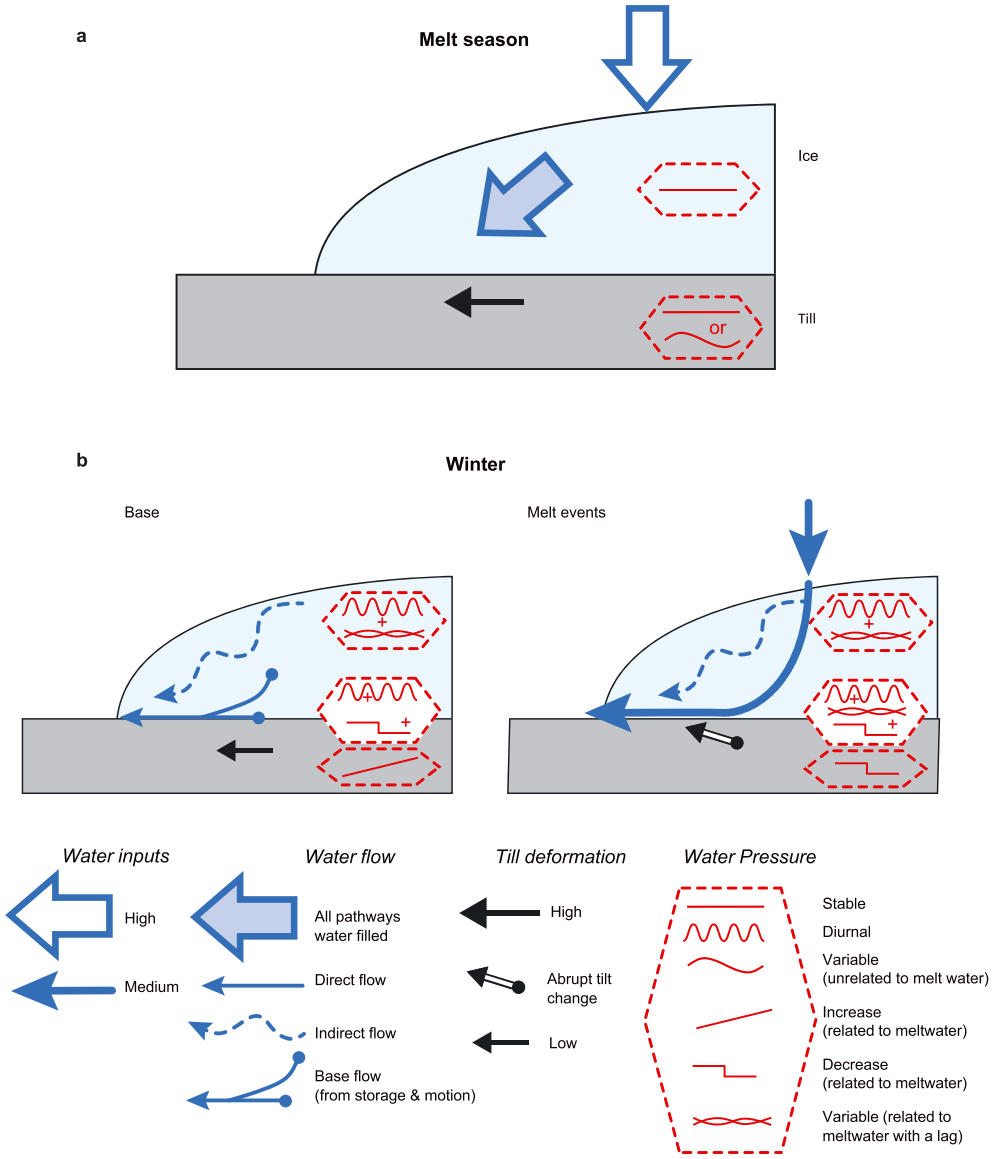

Figure 7. Schematic diagram to show water pathways during the melt season and winter. [Colour figure can be viewed at wileyonlinelibrary.com]

system, and took five days to reach maximum water pressure [similar slow delivery systems have been described by Pohjola, 1993, Murray *et al.*, 2000, Wilson *et al.*, 2013 and Schoof *et al.*, 2014 who described a summer two day lag]. This could be fed from smaller elements such as cracks which can act as englacial storage systems (Schoof *et al.*, 2014). Similar reports of the co-existence of fast and slow drainage have come from Storglaciären, Sweden (Gulley *et al.*, 2009) that had a fast conduit system (Hooke *et al.*, 1988) combined with a slow fracture system (Fountain *et al.*, 2005). We were able to show that during larger melt events, proportionally more of this water was channelled directly to the bed rather than feeding the slow englacial system. This may be because increased surface discharge led to the opening of the larger crevases and moulins.

During the negative degree days ('base' behaviour), water was generated from storage and/or from the frictional heat from glacier movement to produce diurnal fluctuations in water pressure, whilst the indirect flow fed from the melt events continued to travel through the glacier. There was also slow deformation in the till (60% of summer rate).

We have no data concerning the ice/sediment interface during the melt season, however during the winter we saw all three water flow patterns. This included, constant diurnal flow, and then a drop in water pressure during the melt event associated with the direct flow, and then a rise in water pressure peaking five days later reflecting the indirect flow. This latter behaviour does not appear to affect the till nor glacier movement.

Comparison with Greenland

We can compare our results to those from Greenland (Smeets *et al.*, 2012; Meierbachtol *et al.*, 2013; van der Wal *et al.*, 2015) who also used a wireless probe in the ice to record water pressure. They showed the water pressure readings from two boreholes 5 m apart had almost identical behaviour. The pattern of water pressure was very different to that seen at Skálafellsjökull. In Greenland, during autumn and winter, water pressure was relatively high and stable and slowly rose over the period, although in autumn and early winter single melt events affected water pressure and velocity. With the arrival of spring, water pressures initially rose to over 100% and then there was an overall decline in velocity over the summer, with some small velocity increases due to strong melt events or lake drainage (Hoffman *et al.*, 2011; Das *et al.*, 2008) before slowly rising as the summer ended. In general, water pressure and melt were inversely related. During summer, there was a diurnal water pressure record, with meltwater peaks at 14:00 and water pressure and velocity peaks at 15:00.

Table IV. Differences between hard-bedded Greenland and soft-bedded Skálafellsjökull

Seasons	Greenland (ice) (Van de Wal et al., 2015)	Skálafellsjökull (ice, till and interface)
Melt season	Abrupt rise (and then fall) in water pressure and velocity increase (spring event)MW > DC Low water pressure = channels MW < DC	High water pressure = distributed system MW ≈ DC
Winter	High water pressure (rising over whole season) = distributed system MW ≈ DC	Abrupt rise (and then fall) in water pressure and velocity increase (speed-up events) MW > DC Low water pressure (rising between melt events) = more channelized MW < DC

Note: MW, melt water; DC, drainage capacity.

This pattern was interpreted as follows (Smeets et al., 2012; Meierbachtol *et al.*, 2013; van der Wal *et al.*, 2015). During spring, warming temperatures caused the meltwater input to be higher than drainage capacity, leading to water pressure rising higher than overburden pressure and resultant basal sliding ('spring event') (Iken *et al.*, 1993; Bartholomew *et al.*, 2011; Cowton *et al.*, 2013). This event is followed by a decrease in water pressure and velocity, indicating the transition into an efficient network of channels (Schoof, 2010). When the channels were active there was a clear diurnal relationship between water pressure, melt and velocity. In autumn when the melt ceased, the relationship between melt, water pressure and velocity became less distinct as the system returned to an inefficient distributed system (Schoof, 2010).

The opposite behaviour was observed at Skálafellsjökull (Table IV). During the summer, water pressure was high in the ice and till, with no diurnal cycle, and was stable in the ice and either stable or variable (unrelated to surface melt) in the till depending on location. During the winter, water pressure was generally lower in the ice, till and ice/till interface.

Using the model of Schoof (2010) as discussed earlier, this would suggest the summer high water pressures reflect an inefficient drainage system, and the winter low pressures a more channelized system. The summer results are corroborated by the modelling and GPR mapping results from the site by Hart *et al*. (2015) which suggested the presence of a subglacial braided system.

Given this, we suggest that at Skálafellsjökull, during summer the meltwater was approximately equivalent to the drainage capacity. The distributed system could easily adapt to changing inputs. During the winter, overall water pressures were lower, but during the positive degree days melt events inputs were greater than the drainage capacity, and these were accompanied by an abrupt rise and then fall in water pressure and speed-up events. During the negative degree days, water pressure did rise (as during the winter in Greenland), but only until the next warm event (rather than the whole season). Surface melt water continued to travel through the glacier with the five day lag (once within the ice), and was released from storage and generated from motion. Once at the bed the water may have flowed through a series of low pressure channels in the till, which were less able to adapt to changes in inputs, hence the more dramatic water pressure changes during winter.

We argue that there is not a simple seasonal change from winter high pressure distributed to summer low pressure channelized drainage but instead the subglacial environment is characterized by a mainly distributed system which may become more channelized during the winter. We have captured the onset of winter (freezing event) when the diurnal water pressure cycle begins, and the subglacial hydrological system becomes very sensitive to melt. However, we were not able to record the opposite (the spring event), when the diurnal water pressure cycles cease and water pressures in the subglacial environment rise.

Relationship to different responses of melt to glacier dynamics

There has recently been a discussion concerning the effect of increased surface melting on glacier dynamics (as discussed in the Introduction), with most researchers from studies in Greenland, suggesting that once a summer subglacial channelized system develops, then additional melt water has little effect (Sundal *et al.*, 2011; Sole *et al.*, 2013; Tedstone *et al.*, 2015).

Our results suggest that we have a summer distributed system dominated by wide anastomosing broad flat channels and thin water sheets (Hock and Hooke, 1993; Creyts and Schoof, 2009; Schroeder *et al.*, 2013). Water from surface melt rapidly reaches the bed and causes velocity increases during both the melt season and the winter (although the latter is more dramatic). Water is stored within the subglacial system rather than englacially (as we recorded low glacier water content), and the distributed system can rapidly adjust to changes in meltwater production. Similarly, Minchew et al. (2016) have argued that soft bedded glaciers, are more sensitive to meltwater production.

However, Andrews *et al*. (2014) and Hoffman *et al*. (2016) have argued that the pattern proposed for the subglacial hydrology for the Greenland ice sheet (discussed earlier) may be more complex. They also stress the importance of a distributed system (alongside a channelized system) during the melt season. They suggest the distributed system beneath a rigid bedded glacier comprises linked cavities, with a low hydraulic conductivity. They suggest that these patches cover approximately 66% of the bed.

Conclusions

We demonstrate the englacial and subglacial process associated with a soft bedded temperate glacier. This glacier has a fast englacial transfer system which leads to immediate changes in the subglacial hydrological system and glacier velocity in response to surface melt. However, there was an additional slow englacial system which had a five day lag between surface event and subsurface response. This slow system also had an effect at the ice/sediment interface, but was not recorded in the till.

The till and the subglacial hydrological system were coupled, and the bed was composed of a mosaic of different bed strengths (Alley, 1993; Hart and Boulton, 1991; van der Meer *et al.*, 2003; Piotrowski *et al.*, 2004). We are able to show the scale of these patches (e.g. deforming bed equals 77% of total area, typically 8 m in length) which remain relatively

constant throughout the five year study period. However, these classifications may be too coarse to reflect the smaller scale differences between stable and variable water pressures, and the continuum of subglacial hydrological patterns which determine stabilization during the winter, which varied each year.

We were able to show that the till deforms throughout the year. Water pressures were normally high during the melt season (due to very high meltwater inputs), but were often more variable during the winter, and were often associated with a distinctive water pressure cycle related to surface melt events.

We were able to contrast our results with those from a rigid bedded glacier in Greenland. We argue that the seasonal behaviour at Skálafellsjökull is very different, instead of the typical high pressure winter distributed system and low pressure summer channelized system we show the opposite. We argue that because there it is a soft bedded system, the subglacial hydrology is dominated by a distributed system that may become more channelized in winter. These systems are very responsive to melt water inputs, particularly in winter.

Acknowledgements—The authors would like to thank the Glacsweb Iceland 2008/2011 and 2012 teams for help with probe development and data collection. Thanks also go to Lyn Aspden and Mark Dover and in the Cartographic Unit for figure preparation. This research was funded by Engineering and Physical Sciences Research Council (EP/C511050/1), Leverhulme Trust (F/00 180/AK) and the National Geographic Society (GEFNE45-12) and the GPR and Leica 1200 GPS units were loaned from the NERC Geophysical Equipment Facility.

References

Alley RB. 1993. In search of ice-stream sticky spots. *Journal of Glaciology* **39**: 447–454.

Alley RB, Blankenship DD, Bentley CR, Rooney S. 1986. Deformation of till beneath ice stream B, West Antarctica. *Nature* **322**(6074): 57–59.

Anderson RS, Anderson SP, MacGregor KR, Waddington ED, O'Neel S, Riihimaki CA, Loso MG. 2004. Strong feedbacks between hydrology and sliding of a small alpine glacier. *Journal of Geophysical Research: Earth Surface* **109**(F3).

Andrews LC, Catania GA, Hoffman MJ, Gulley JD, Lüthi MP, Ryser C, Hawley RL, Neumann TA. 2014. Direct observations of evolving subglacial drainage beneath the Greenland Ice Sheet. *Nature* **514**(7520): 80.

Bartholomew I, Nienow P, Mair D, Hubbard A, King MA, Sole A. 2010. Seasonal evolution of subglacial drainage and acceleration in a Greenland outlet glacier. *Nature Geoscience* **3**(6): 408.

Bartholomew I, Nienow P, Sole A, Mair D, Cowton T, Palmer S, Wadham J. 2011. Supraglacial forcing of subglacial drainage in the ablation zone of the Greenland ice sheet. *Geophysical Research Letters* **38**(8).

Bartholomew I, Nienow P, Sole A, Mair D, Cowton T, King MA. 2012. Short-term variability in Greenland Ice Sheet motion forced by time-varying meltwater drainage: Implications for the relationship between subglacial drainage system behavior and ice velocity. *Journal of Geophysical Research: Earth Surface* **117**(F3).

Blake EW, Clarke GKC, Gerrin MC. 1992. Tools for examining subglacial bed deformation. *Journal of Glaciology* **38**: 388–396.

Boulton GS, Hindmarsh RCA. 1987. Sediment deformation beneath glaciers: rheology and geological consequences. *Journal of Geophysical Research: Solid Earth* **92**(B9): 9059–9082.

Boulton GS, Jones AS. 1979. Stability of temperate ice caps and ice sheets resting on beds of deformable sediment. *Journal of Glaciology* **24**: 29–43.

Boulton GS, Dobbie KE, Zatsepin S. 2001. Sediment deformation beneath glaciers and its coupling to the subglacial hydraulic system. *Quaternary International* **86**: 3–28.

Braithwaite RJ. 1995. Positive degree-day factors for ablation on the Greenland Ice-sheet studied by energy-balance modelling. *Journal of Glaciology* **41**: 153–160.

Brown NE, Hallet B, Booth DB. 1987. Rapid soft bed sliding of the Puget Glacier lobe. *Journal of Geophysical Research* **92**(B9): 8985–8997.

Clarke GKC. 1987. Subglacial till: a physical framework for its properties and processes. *Journal of Geophysical Research: Solid Earth* **92**(B9): 9023–9036.

Cohen J, Screen JA, Furtado JC, Barlow M, Whittleston D, Coumou D, Francis J, Dethloff K, Entekhabi D, Overland J, Jones J. 2014. Recent Arctic amplification and extreme mid-latitude weather. *Nature Geoscience* **7**(9): 627.

Cowton T, Nienow P, Sole A, Wadham J, Lis G, Bartholomew I, Mair D, Chandler D. 2013. Evolution of drainage system morphology at a land-terminating Greenlandic outlet glacier. *Journal of Geophysical Research: Earth Surface* **118**(1): 29–41.

Creyts TT, Schoof CG. 2009. Drainage through subglacial water sheets. *Journal of Geophysical Research: Earth Surface* **114**(F4).

Das SB, Joughin I, Behn MD, Howat IM, King MA, Lizarralde D, Bhatia MP. 2008. Fracture propagation to the base of the Greenland Ice Sheet during supraglacial lake drainage. *Science* **320**(5877): 778–781.

DeConto RM, Pollard D. 2016. Contribution of Antratica to past and future sea-level rise. *Nature* **531**: 591–597.

Fischer UH, Clarke GKC. 2001. Review of subglacial hydro-mechanical coupling: Trapridge glacier, Yukon Territory, Canada. *Quaternary International* **86**(1): 29–43.

Fountain AG, Walder JS. 1998. Water flow through temperate glaciers. *Reviews of Geophysics* **36**(3): 299–328.

Fountain AG, Jacobel RW, Schlichting R, Jansson P. 2005. Fractures as the main pathways of water flow in temperate glaciers. *Nature* **433**(7026): 618–621.

Gades AM, Raymond CF, Conway H, Jacobel RW. 2000. Bed properties of Siple Dome and adjacent ice streams, West Antarctica, inferred from radio-echo sounding measurements. *Journal of Glaciology* **46**(152): 88–94.

Gooseff MN, McKnight DM, Lyons WB, Blum AE. 2002. Weathering reactions and hyporheic exchange controls on stream water chemistry in a glacial meltwater stream in the McMurdo Dry Valleys. *Water Resources Research* **38**(12).

Gulley JD, Benn DI, Screaton E, Martin J. 2009. Mechanisms of englacial conduit formation and their implications for subglacial recharge. *Quaternary Science Reviews* **28**(19): 1984–1999.

Harper JT, Humphrey NF. 1995. Borehole video analysis of a temperate glacier'englacial and subglacial structure: Implications for glacier flow models. *Geology* **23**(10): 901–904.

Hart JK, Boulton GS. 1991. The interrelation of glaciotectonic and glaciodepositional processes within the glacial environment. *Quaternary Science Reviews* **10**(4): 335–350.

Hart JK, Martinez K. 2006. Environmental sensor networks: a revolution in the earth system science? *Earth-Science Reviews* **78**(3): 177–191.

Hart JK, Rose KC, Martinez K, Ong R. 2009. Subglacial clast behaviour and its implication for till fabric development: new results derived from wireless subglacial probe experiments. *Quaternary Science Reviews* **28**(7): 597–607.

Hart JK, Rose KC, Martinez K. 2011. Subglacial till behaviour derived from in situ wireless multi-sensor subglacial probes: rheology, hydro-mechanical interactions and till formation. *Quaternary Science Reviews* **30**(1): 234–247.

Hart JK, Rose KC, Clayton A, Martinez K. 2015. Englacial and subglacial water flow at Skálafellsjökull, Iceland derived from ground penetrating radar, in situ Glacsweb probe and borehole water level measurements. *Earth Surface Processes and Landforms* **40**(15): 2071–2083.

Hart JK, Clayton AI, Martinez K, Robson BA. 2018. Erosional and depositional subglacial streamlining processes at Skálafellsjökull, Iceland: an analogue for a new bedform continuum model. *GFF*: 1–17.

Hicock SR. 1992. Lobal interactions and rheologic superposition in subglacial till near Bradtville, Ontario, Canada. *Boreas* **21**(1): 73–88.

Hicock SR, Dreimanis A. 1992. Deformation till in the Great Lakes region: implications for rapid flow along the south-central margin of the Laurentide Ice Sheet. *Canadian Journal of Earth Sciences* **29**(7): 1565–1579.

Hock R. 2003. Temperature index temperature modelling in mountain areas. *Journal of Hydrology* **282**: 104–115.

Hock R, Hooke RL. 1993. Evolution of the internal drainage system in the lower part of the ablation area of Storglaciären, Sweden. *Geological Society of America Bulletin* **105**: 537–546.

Hodge SM. 1976. Direct measurement of basal water pressures: a pilot study. *Journal of Glaciology* **16**(74): 205–218.

Hoffman MJ, Catania GA, Neumann TA, Andrews LC, Rumrill JA. 2011. Links between acceleration, melting, and supraglacial lake drainage of the western Greenland Ice Sheet. *Journal of Geophysical Research: Earth Surface* **116**(F4).

Hoffman MJ, Andrews LC, Price SF, Catania GA, Neumann TA, Lüthi MP, Gulley J, Ryser C, Hawley RL, Morriss B. 2016. Greenland subglacial drainage evolution regulated by weakly connected regions of the bed. *Nature Communications* **7**: 13903.

Hooke RL, Miller SB, Kohler J. 1988. Character of the englacial and sub-glacial drainage system in the upper part of the ablation area of Storglaciaren, Sweden. *Journal of Glaciology* **34**(117): 228–231.

Hooke RL, Laumann T, Kohler J. 1990. Subglacial water pressures and the shape of subglacial conduits. *Journal of Glaciology* **36**(122): 67–71.

Hubbard B, Nienow P. 1997. Alpine subglacial hydrology. *Quaternary Science Reviews* **16**(9): 939–955.

Hubbard BP, Sharp MJ, Willis IC, Nielsen MT, Smart CC. 1995. Borehole water-level variations and the structure of the subglacial hydrological system of Haut Glacier d'Arolla, Valais, Switzerland. *Journal of Glaciology* **41**(139): 572–583.

Hubbard B, Roberson S, Samyn D, Merton-Lyn D. 2008. Digital optical televiewing of ice boreholes. *Journal of Glaciology* **54**(188): 823–830.

Iken A, Echelmeyer K, Harrison W, Funk M. 1993. Mechanisms of fast flow in Jakobshavn Isbræ, West Greenland: Part I. Measurements of temperature and water level in deep boreholes. **39**(131): 15–25.

Iverson NR. 2010. Shear resistance and continuity of subglacial till: hydrology rules. *Journal of Glaciology* **56**(200): 1104–1114.

Jacobel RW, Welch BC, Osterhouse D, Pettersson R, MacGregor JA. 2009. Spatial variation of radar-derived basal conditions on Kamb Ice Stream. *Annals of Glaciology* **50**(51): 10–16.

Jacobel RW, Lapo KE, Stamp JR, Youngblood BW, Welch BC, Bamber JL. 2010. Comparison of basal reflectivity and ice velocity in east Antarctica. *The Cryosphere* **4**: 447–452.

Johannesson T, Sigurdsson O, Laumann T, Kennett M. 1995. Degree-day glacier mass-balance modelling with applications to glaciers in Iceland, Norway and Greenland. *Journal of Glaciology* **41**(138): 345–358.

Joughin I, Das SB, King MA, Smith BE, Howat IM, Moon T. 2008. Seasonal speedup along the western flank of the Greenland Ice Sheet. *Science* **320**(5877): 781–783.

Joughin I, Smith BE, Medley B. 2014. Marine ice sheet collapse potentially under way for the Thwaites Glacier Basin, West Antarctica. *Science* **344**(6185): 735–738.

Kamb B. 1991. Rheological nonlinearity and flow instability in the deforming bed mechanism of ice stream motion. *Journal of Geophysical Research: Solid Earth* **96**(B10): 16585–16595.

Kavanaugh JL, Clarke GKC. 2001. Abrupt glacier motion and reorganization of basal shear stress following the establishment of a connected drainage system. *Journal of Glaciology* **47**(158): 472–480.

King EC, Hindmarsh RC, Stokes CR. 2009. Formation of mega-scale glacial lineations observed beneath a West Antarctic ice stream. *Nature Geoscience* **2**(8): 585–588.

MacGregor JA, Winebrenner DP, Conway H, Matsuoka K, Mayewski PA, Clow GD. 2007. Modeling englacial radar attenuation at Siple Dome, West Antarctica, using ice chemistry and temperature data. *Journal of Geophysical Research* **112**: F03008. https://doi.org/10.1029/2006JF000717.

Martinez K, Hart JK, Ong R. 2009. Deploying a wireless sensor network in Iceland. In *GeoSensor Networks*. Springer: Berlin; 131–137.

Martinez K, Basford PJ, De Jager D, Hart JK. 2012. A wireless sensor network system deployment for detecting stick slip motion in glaciers. In *Wireless Sensor Systems (WSS 2012)*. IET Conference; 1–3.

Matsuoka K, Morse D, Raymond CF. 2010. Estimating englacial radar attenuation using depth profiles of the returned power, Central West Antarctica. *Journal of Geophysical Research* **115**: F02012. https://doi.org/10.1029/2009JF001496.

Meierbachtol T, Harper J, Humphrey N. 2013. Basal drainage system response to increasing surface melt on the Greenland Ice Sheet. *Science* **341**(6147): 777–779.

Minchew B, Simons M, Björnsson H, Pálsson F, Morlighem M, Seroussi H, Larour E, Hensley S. 2016. Plastic bed beneath Hofsjökull Ice Cap, central Iceland, and the sensitivity of ice flow to surface meltwater flux. *Journal of Glaciology* **62**(231): 147–158.

Moorman BJ, Michel FA. 2000. Glacial hydrological system characterization using ground-penetrating radar. *Hydrological Processes* **14**(15): 2645–2667.

Murray T, Clarke GKC. 1995. Black-box modelling of the subglacial water system. *Journal of Geophysical Research* **100**(B6): 10231–10245. https://doi.org/10.1029/95JB00671.

Murray T, Porter PR. 2001. Basal conditions beneath a soft-bedded polythermal surge-type glacier: Bakaninbreen, Svalbard. *Quaternary International* **86**(1): 103–116.

Murray T, Stuart GW, Fry M, Gamble NH, Crabtree MD. 2000. Englacial water distribution in a temperate glacier from surface and bore hole radar velocity analysis. *Journal of Glaciology* **46**(154): 389–398.

Nienow P, Sharp M, Willis I. 1998. Seasonal changes in the morphology of the subglacial drainage system, Haut Glacier d'Arolla, Switzerland. *Earth Surface Processes and Landforms* **23**(9): 825–843.

Nienow PW, Hubbard AL, Hubbard BP, Chandler DM, Mair DWF, Sharp MJ, Willis IC. 2005. Hydrological controls on diurnal ice flow variability in valley glaciers. *Journal of Geophysical Research* **110**: F04002. https://doi.org/10.1029/2003JF000112.

Piotrowski JA, Larsen NK, Junge FW. 2004. Reflections on soft subglacial beds as a mosaic of deforming and stable spots. *Quaternary Science Reviews* **23**: 993–1000.

Pohjola VA. 1993. TV-video observations of bed and basal sliding on Storglaciären, Sweden. *Journal of Glaciology* **39**(131): 111–118.

Pohjola VA. 1994. TV-video observations of englacial voids in Storglaciären, Sweden. *Journal of Glaciology* **40**(135): 231–240.

Raymond CF, Harrison WD. 1975. Some observations on the behavior of the liquid and gas phases in temperate glacier ice. *Journal of Glaciology* **14**(71): 213–233.

Rennermalm AK, Smith LC, Chu VW, Box JE, Forster RR, Van den Broeke MR, Van As D, Moustafa SE. 2013. Evidence of meltwater retention within the Greenland Ice Sheet. *The Cryosphere* **7**: 1433–1445.

Röthlisberger H. 1972. Water pressure in intra-and subglacial channels. *Journal of Glaciology* **11**(62): 177–203.

Schoof C. 2010. Ice-sheet acceleration driven by melt supply variability. *Nature* **468**(7325): 803.

Schoof C, Rada CA, Wilson NJ, Flowers GE, Haseloff M. 2014. Oscillatory subglacial drainage in the absence of surface melt. *The Cryosphere* **8**(3): 959–976.

Schroeder DM, Blankenship DD, Young DA. 2013. Evidence for a water system transition beneath Thwaites Glacier, West Antarctica. *Proceedings of the National Academy of Sciences of the United States of America* **110**: 12225–12228.

Serreze MC, Francis JA. 2006. The Arctic amplification debate. *Climatic Change* **76**: 241–264.

Shepherd A, Hubbard A, Nienow P, King M, McMillan M, Joughin I. 2009. Greenland Ice Sheet motion coupled with daily melting in late summer. *Geophysical Research Letters* **36**(1).

Sigurðsson O. 1998. Glacier variations in Iceland 1930–1995. *Jökull* **45**: 3–25.

Smeets CJPP, Boot W, Hubbard A, Pettersson R, Wilhelms F, Van Den Broeke MR, Van De Wal RS. 2012. A wireless subglacial probe for deep ice applications. *Journal of Glaciology* **58**(211): 841–848.

Smith AM. 2006. Microearthquakes and subglacial conditions. *Geophysical Research Letters* **33**: L24501. https://doi.org/10.1029/2006GL028207.

Smith AM, Murray T. 2009. Bedform topography and basal conditions beneath a fast-flowing West Antarctic ice stream. *Quaternary Science Reviews* **28**(7): 584–596.

Sole A, Nienow P, Bartholomew I, Mair D, Cowton T, Tedstone A, King MA. 2013. Winter motion mediates dynamic response of the Greenland Ice Sheet to warmer summers. *Geophysical Research Letters* **40**(15): 3940–3944.

Solomon S et al. (eds). 2007. *Climate Change 2007: The Physical Science Basis*. Cambridge University Press: Cambridge.

Stokes CR, Clark CD, Lian OB, Tulaczyk S. 2007. Ice stream sticky spots: a review of their identification and influence beneath contemporary and palaeo-ice streams. *Earth-Science Reviews* **81**(3): 217–249.

Stokes CR, Clark CD, Storrar R. 2009. Major changes in ice stream dynamics during deglaciation of the north-western margin of the Laurentide Ice Sheet. *Quaternary Science Reviews* **28**(7): 721–738.

Sugiyama S, Skvarca P, Naito N, Enomoto H, Tsutaki S, Tone K, Marinsek S, Aniya M. 2011. Ice speed of a calving glacier modulated by small fluctuations in basal water pressure. *Nature Geoscience* **4**: 597–600.

Sundal AV, Shepherd A, Nienow P, Hanna E, Palmer S, Huybrechts P. 2011. Melt-induced speed-up of Greenland ice sheet offset by efficient subglacial drainage. *Nature* **469**(7331): 521.

Tedstone AJ, Nienow PW, Gourmelen N, Dehecq A, Goldberg D, Hanna E. 2015. Decadal slowdown of a land-terminating sector of the Greenland Ice Sheet despite warming. *Nature* **526**(7575): 692.

Trommelen MS, Ross M, Ismail A. 2014. Ribbed moraines in northern Manitoba, Canada: characteristics and preservation as part of a subglacial bed mosaic near the core regions of ice sheets. *Quaternary Science Reviews* **87**: 135–155.

van der Wal RSW, Smeets CJPP, Boot W, Stoffelen M, Van Kampen R, Doyle SH, Wilhelms F, Van den Broeke MR, Reijmer CH, Oerlemans J, Hubbard A. 2015. Self-regulation of ice flow varies across the ablation area in south-west Greenland. *The Cryosphere* **9**(2): 603–611.

van der Meer JJ, Menzies J, Rose J. 2003. Subglacial till: the deforming glacier bed. *Quaternary Science Reviews* **22**(15): 1659–1685.

Waechter A, Copland L, Herdes E. 2015. Modern glacier velocities across the Icefield Ranges, St Elias Mountains, and variability at selected glaciers from 1959 to 2012. *Journal of Glaciology* **61**(228): 624–634.

Walder JS, Fowler A. 1994. Channelized subglacial drainage over a deformable bed. *Journal of Glaciology* **40**: 3–15.

Weertman J. 1964. The theory of glacier sliding. *Journal of Glaciology* **5**(39): 287–303.

Wiens DA, Anandakrishnan S, Winberry JP, King MA. 2008. Simultaneous teleseismic and geodetic observations of the stick–slip motion of an Antarctic ice stream. *Nature* **453**(7196): 770–774.

Willis IC. 1995. Interannual variations in glacier motion – a review. *Progress in Physical Geography* **19**: 61–106.

Wilson N, Flowers G, Mingo L. 2013. Characterization and interpretation of polythermal structure in two subarctic glaciers. *Journal of Geophysical Research* **118**: 1443–1459. https://doi.org/10.1002/jgrf.20096.

Winebrenner DP, Smith BE, Catania GA, Conway HB, Raymond CF. 2003. Radio-frequency attenuation beneath Siple Dome, West Antarctica, from wide-angle and profiling radar observations. *Annals of Glaciology* **37**: 226–232.

Young DS, Hart JK, Martinez K. 2015. Image analysis techniques to estimate river discharge using time-lapse cameras in remote locations. *Computers & Geosciences* **76**: 1–10.

Zwally HJ, Abdalati W, Herring T, Larson K, Saba J, Steffen K. 2002. Surface melt-induced acceleration of Greenland ice-sheet flow. *Science* **297**(5579): 218–222.